The Adoption of AISC 360 for Offshore Structural Design Practices

ALBERT KU, FARREL ZWERNEMAN, STEVE GUNZELMAN, and JIEYAN CHEN

ABSTRACT

The offshore design standards for U.S. practices refer to AISC specifications when designing structural components with nontubular shapes. The widely used API RP-2A WSD standard (API, 2014) asks designers to use the 1989 AISC *Specification* (AISC, 1989a). The newly published API RP-2A LRFD (API, 2019) and RP-2TOP (ANSI/API, 2019) ask designers to use the 2010 AISC *Specification* (AISC, 2010). Although the 2010 AISC *Specification* has been partially adopted by API, the current offshore practice is still primarily dominated by the 1989 AISC *Specification*. The key issue hampering the offshore community's full adoption of the 2010 AISC *Specification* is the relative ease of accounting for second-order effects in the 1989 AISC *Specification*. In 2019, API formed a Task Group dedicated to studying this issue, with the main findings summarized in this paper. By illustrating the key code check process in two examples with an easy-to-understand format, this paper aims at assisting the offshore structural engineers to better understand the latest AISC *Specification*. The authors also hope that this paper will serve as a communication path between the offshore structural community and AISC for current and future standards' adoption and harmonization.

Keywords: offshore structural design, topsides structural design, API RP-2A, API RP-2TOP.

INTRODUCTION

For the offshore industry, use of the 1989 AISC *Specification for Structural Steel Buildings* (AISC, 1989a) together with the 9th Edition *Steel Construction Manual* (AISC, 1989b) has been a long-held tradition. When the American Petroleum Institute (API) issued the most recent working stress design (WSD) standard—the API RP-2A WSD, 22nd Edition (API, 2014), in 2014—use of the AISC *Specification for Structural Steel Buildings*, ANSI/AISC 360, hereafter referred to as AISC 360, was explicitly discouraged in both the Foreword and Section 6.1.1 of that API document. The fundamental reason for API's hesitation to adopt AISC 360 has been a lack of sufficient understanding on the new frame stability provisions, and its associated second-order analysis concept. It is our hope that this paper will benefit other offshore structural engineers who wish to understand the issues of transitioning from the 1989 AISC *Specification* to AISC 360-16 (AISC, 2016).

Albert Ku, PhD, PE, Principal Engineer, DNV Energy Systems, New Taipei City, Taiwan. Email: albert.ku@dnv.com (corresponding)

Farrel Zwerneman, Independent Consultant, Houston, Tex. Email: fzwern0@gmail.com

Steve Gunzelman, Independent Consultant, Houston, Tex. Email: gunzclan@earthlink.net

Jieyan Chen, Structural Engineer, IntelliSIMS, Houston, Tex. Email: jieyan@intellisims.com

Paper No. 2023-04

On AISC's frame stability procedure, excellent references can be found in AISC Design Guide 28, *Stability Design of Steel Buildings* (Griffis and White, 2013), the summary paper by Carter and Geschwindner (2008), the summary note by Carter (2013), and the SSRC *Stability Guide* (Ziemian, 2010). The lead author of this paper found Carter and Geschwindner (2008) to be particularly lucid and benefited with a good understanding of the AISC 360 frame stability process after reading that work. In this paper, we attempt to follow the same style by giving simple examples with clear explanations on the calculation process. In addition, the comparison paper between the AISC *Specification* and Eurocode 3 by Bernuzzi et. al. (2015) is also of note.

It should be noted that API did adopt a version of AISC 360 [AISC 360-10, which corresponds to the 14th Edition *Manual* (AISC, 2011)] in 2019 with the publication of API RP-2TOP (ANSI/API, 2019). The 2016 AISC *Specification*, AISC 360-16, was not adopted because the 2TOP draft was prepared before 2016. Although the API RP-2TOP document adopts AISC 360-10, this AISC *Specification* and its associated frame stability concept are still foreign to most offshore structural engineers. Its relation to tubular structural designs, which form the core of API RP-2A WSD and RP-2A LRFD, are also not well understood.

The first offshore platform was installed in 1948 in the Gulf of Mexico. In the early years of offshore oil and gas platform design, construction, and installation, there were no specific standards applicable to this industry. Offshore structural engineers had to rely on onshore steel structure experiences and the standards as published by AISC. The 1st Edition API RP-2A design standard, *API Recommended*

Practice for Planning, Designing, and Constructing Fixed Offshore Platforms, was published in 1969 with 16 pages (API, 1969). In the span of 45 years (1969–2014), there would be 21 more editions of API RP-2A based on the working stress design (WSD) concept, with the latest, API RP-2A WSD 22nd Edition (2014), expanded to 310 pages. Throughout these editions, the connection to AISC *Specifications* has been important. The connection lies in the adopted equations (for tubular member design use) and its explicit requirement to use AISC *Specifications* for non-tubular member designs.

API published its first LRFD-based RP-2A in 1993 (API, 1993), and in this standard, the connection to the 1986 AISC LRFD *Specification* (AISC, 1986) was referenced. However, the use of this LRFD standard had been very limited in the United States, and the offshore industry continued to be dominated by the WSD design practice. API retracted the 1st Edition API 2A-LRFD in 2012 due to a lack of technical maintenance. This standard was upgraded and reissued in 2019 as the API RP-2A LRFD 2nd Edition (API, 2019). Whether the use of this new LRFD standard will be more widespread remains to be seen.

Fixed offshore structures are typically completely braced, as shown on the left side of Figure 1. In some geographical areas with low seismicity, such as the Gulf of Mexico, many jackets have a "portal bay" in between the jacket and topsides (i.e., deck) as shown on the right side of Figure 1. This can be due to installation requirements or a desire to reduce the wave load in the splash zone. This portal bay will experience the second-order effect (P-Δ effect) the most, when compared to other braced parts of the structure. In addition, equipment support modules on the topsides can be unbraced. Designers for these two types of structure—namely, the jacket portal bay and the unbraced equipment support module—should be keenly aware of the latest AISC standard requirement related to frame stability.

From the authors' point of view, the differences between the AISC 1989 *Specification* and AISC 360-16 are primarily in the beam-column code check, and the types of structural analysis required for that check. This is summarized in Table 1. For code checks using the 1989 *Specification*, the structural analysis should be first-order based. The beam-column equation in the 1989 *Specification* contains a magnification factor on the bending stress to represent the second-order effect.

For code checks using AISC 360-16, the structural analysis should be second-order based. Because the structural load demands obtained from the analyses already include the second-order effect, the beam-column equations no longer require a magnification factor.

In AISC 360-16, three types of frame stability analysis can be employed: the effective-length method (ELM), the direct-analysis method (DM), and the first-order method (FOM). A summary is shown in Table 2. The detailed discussions on these methods will be postponed until the examples are presented.

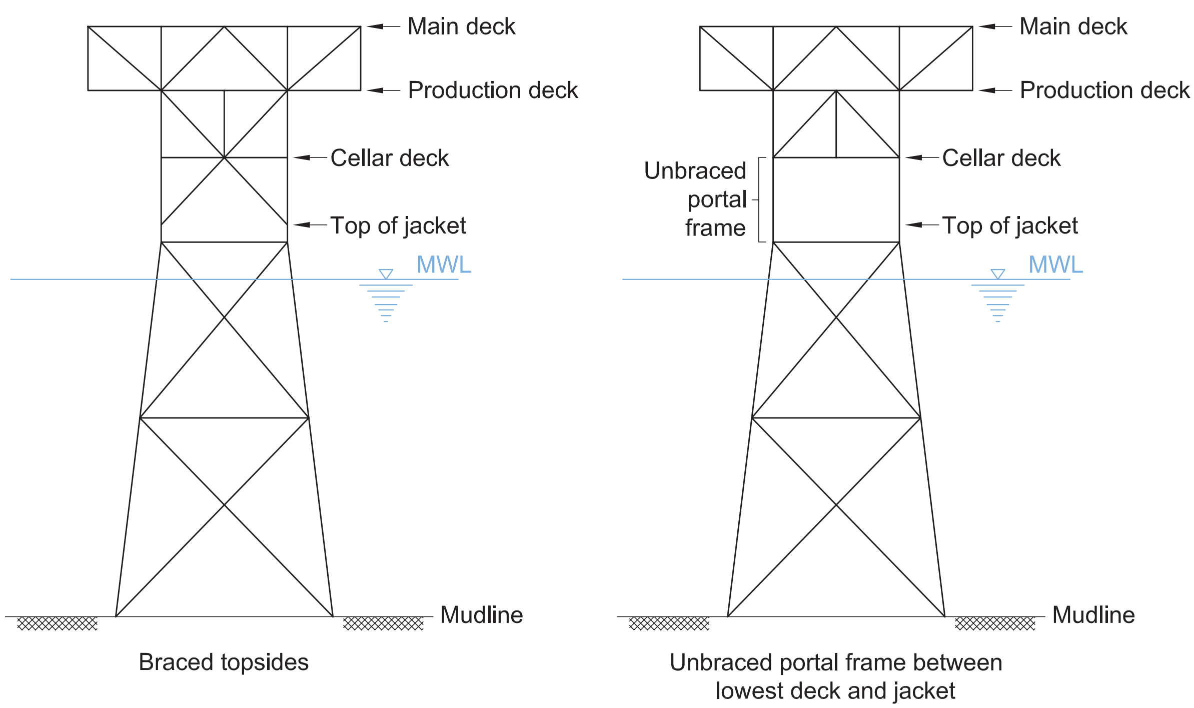

Fig. 1. Braced offshore structure (left) and partially braced with portal bay (right).

Table 1. Summary of the Beam-Column Check for the AISC 1989 and 2016 *Specifications*		
	AISC 1989 *Specification*	AISC 2016 *Specification*
Structural analysis method	First-order based	Second-order based
Beam-column unity check equation	$\frac{f_a}{F_a}+\frac{C_{mx}f_{bx}}{\left(1-\frac{f_a}{F'_{ex}}\right)F_{bx}}+\frac{C_{my}f_{by}}{\left(1-\frac{f_a}{F'_{ey}}\right)F_{by}}\leq 1.0^{(1)}$ Second-order magnified	$\frac{P_r}{P_c}+\frac{8}{9}\left(\frac{M_{rx}}{M_{cx}}+\frac{M_{ry}}{M_{cy}}\right)\leq 1.0^{(2)}$ No magnification

Notes: (1): Only the buckling equation is shown
(2): For the $P_r/P_c > 0.2$ segment

In this paper, two examples are considered: a cantilever beam-column and a two-dimensional structure with a portal bay. In the cantilever example, two levels of horizontal load are examined. Offshore structures are subjected to lateral loads from wind, wave, and current, and they are checked in combination with gravity loads. A lateral-to-vertical load ratio of 2% is on the low side; the more typical ratio will be 5% or higher. A structural member designed to the 5% lateral-to-vertical ratio will have a higher bending code check component (and lower axial component) than the 2% lateral-to-vertical case. Since the second-order effect is strongly associated with the P-Δ effect, the 5% case with the lower axial load will have a lower second-order effect. This will reflect on their B_2 values to be discussed later.

In the cantilever example, unity code check values for the 2% and 5% lateral-to-vertical load ratios are both examined. Although 5% is the more typical case for offshore structures, in the 2D structure example, only the 2% case will be given. This is due to the paper's length limit, as well as that the 2% case will generate higher second-order effects. Consequently, these results are more interesting for frame stability considerations. The code checks performed in this paper are ASD or WSD checks with no additional allowable stress increase. The cases examined are summarized in Table 3.

CAPACITY EQUATIONS

Capacity equations can be found in the AISC *Specification*, Section E for compression, Section F for flexure, and Section H for beam-columns. In this section of the paper, only the general forms of these equations are listed for the purpose of explaining code check procedures. Refer to AISC 360-16 (AISC, 2016) and the 1989 AISC *Specification* (1989a), for equation details and associated notations. In the following, the equation numbers from the original references are also listed.

AISC 1989 *Specification*

The beam-column checks must satisfy the following two equations, with the first equation related to buckling and the second equation related to yielding. Both equations need to be satisfied.

$$\frac{f_a}{F_a}+\frac{C_{mx}f_{bx}}{\left(1-\frac{f_a}{F'_{ex}}\right)F_{bx}}+\frac{C_{my}f_{by}}{\left(1-\frac{f_a}{F'_{ey}}\right)F_{by}}\leq 1.0 \tag{1}$$
Spec. Eq. H1-1

$$\frac{f_a}{0.6F_y}+\frac{f_{bx}}{F_{bx}}+\frac{f_{by}}{F_{by}}\leq 1.0 \tag{2}$$
Spec. Eq. H1-2

The allowable axial compression stress is:

$$F_a=\begin{cases}\dfrac{\left[1-\dfrac{(KL/r)^2}{2C_c^2}\right]F_y}{\dfrac{5}{3}+\dfrac{3(KL/r)}{8C_c}-\dfrac{(KL/r)^3}{8C_c^3}}, & \dfrac{(KL/r)}{C_c}\leq 1.0 \\ \dfrac{12\pi^2E}{23(KL/r)^2}, & \dfrac{(KL/r)}{C_c}>1.0\end{cases} \tag{3}$$
Spec. Eq. E2-1
Spec. Eq. E2-2

The allowable bending stress of I-shaped members is:

$$F_b=0.66F_y \qquad L_b\leq L_c \tag{4}$$
Spec. Eq. F1-1

L_c is given by:

$$L_c=\min\left\{\frac{76b_f}{\sqrt{F_y}},\ \frac{20{,}000}{(d/A_f)F_y}\right\} \tag{5}$$
Spec. Eq. F1-2

When the unbraced length is greater than L_c, the allowable bending stress is:

Table 2. Summary of ELM, DM, and FOM			
	Effective-Length Method (ELM)	**Direct-Analysis Method (DM)**	**First-Order Method (FOM)**
Limitation	$B_2 = \dfrac{\Delta_{2nd}}{\Delta_{1st}} \le 1.5$ (Δ = average story drift)	None(1)	$B_2 \le 1.5$, $\dfrac{\alpha P_r}{P_y} \le 0.5$
Analysis type	Second-order elastic	Second-order elastic	First-order elastic
Notional lateral loads(4)	$N_i = 0.002Y_i$, minimum(3) (Y_i = gravity load applied at level i, LRFD or 1.6 times the ASD load combinations)	$N_i = 0.002Y_i$ (minimum lateral load if $B_2 \le 1.5$; additive if $B_2 > 1.5$)	$N_i = 2.1\left(\dfrac{\Delta}{L}\right)Yi \ge 0.0042\left(\dfrac{Y_i}{\alpha}\right)$ additive(3)
Member stiffness	Nominal EA, EI	Reduced $EA^* = 0.8\tau_b EA$, $EI^* = 0.8EI$ $\tau_b{}^{(2)} = \begin{cases} 1.0 \text{ when } \alpha P_r/P_y \le 0.5 \\ 4(\alpha P_r/P_y)\left[1-(\alpha P_r/P_y)\right]^{(5)} \end{cases}$	Nominal EA, EI
K factor	Buckling analysis from API/AISC guidance	$K = 1.0$	$K = 1.0$

Notes: (1) Though DM can apply to high B_2, it is recommended to limit $B_2 \le 1.5$ for offshore design as a rule.
(2) In DM, EA and EI are reduced by 20% to represent cross-sectional premature yielding due to residual stress. If axial load is high $(\alpha P_r/P_y) > 0.5$, cross-sectional stiffness is further reduced by τ_b.
(3) Minimum: if actual applied loads are greater, N_i is ignored. Additive: N_i is applied regardless of actual lateral load.
(4) Notional lateral loads for ELM and DM are meant to represent initial out-of-plumbness. Notional lateral loads for FOM are meant to represent second-order load effect with a first-order structural analysis.
(5) τ_b can be taken as 1.0 in all members if additional notional loads of $0.001Y_i$ are applied to lateral loads.

Table 3. Code Check Cases Performed in This Study		
	Cantilever	**2D Jacket**
H* = 5%*P		
AISC 1989 *Specification*	√	—
AISC 360-16 ELM	√	—
AISC 360-16 DM	—	—
AISC 360-16 FOM	—	—
H* = 2%*P		
AISC 1989 *Specification*	√	√
AISC 360-16 ELM	√	√
AISC 360-16 DM	—	√
AISC 360-16 FOM	—	√

$$F_b = \begin{cases} \left[\dfrac{2}{3} - \dfrac{F_y\left(L_b/r_T\right)^2}{1530\times10^3 C_b}\right]F_y \le 0.60F_y, & \sqrt{\dfrac{102\times10^3 C_b}{F_y}} \le \dfrac{L_b}{r_T} \le \sqrt{\dfrac{510\times10^3 C_b}{F_y}} \\ \dfrac{170\times10^3 C_b}{\left(L_b/r_T\right)^2} \le 0.60F_y, & \dfrac{L_b}{r_T} > \sqrt{\dfrac{510\times10^3 C_b}{F_y}} \end{cases} \tag{6}$$

Spec. Eq. F1-6
Spec. Eq. F1-7

AISC 360-16

Beam-column checks must satisfy the following two equations. These two equations are in fact one equation but with different slopes on the *P-M* interaction diagram:

$$\frac{P_r}{P_c} + \frac{8}{9}\left(\frac{M_{rx}}{M_{cx}} + \frac{M_{ry}}{M_{cy}}\right) \le 1.0, \quad \frac{P_r}{P_c} \ge 0.2 \tag{7}$$

Spec. Eq. H1-1a

$$\frac{P_r}{2P_c} + \left(\frac{M_{rx}}{M_{cx}} + \frac{M_{ry}}{M_{cy}}\right) \le 1.0, \quad \frac{P_r}{P_c} < 0.2 \tag{8}$$

Spec. Eq. H1-1b

The nominal axial strength is as follows:

$$P_n = F_{cr} A_g \tag{9}$$

Spec. Eq. E3-1

$$F_{cr} = \begin{cases} \left(0.658^{\frac{F_y}{F_e}}\right)F_y, & \dfrac{F_y}{F_e} \le 2.25 \\ 0.877F_y, & \dfrac{F_y}{F_e} > 2.25 \end{cases} \tag{10}$$

Spec. Eq. E3-2
Spec. Eq. E3-3

The nominal flexural strength is as follows:

$$M_n = \begin{cases} M_p = F_y Z_x, & L_b \le L_p \\ C_b\left[M_p - \left(M_p - 0.75F_y S_x\right)\left(\dfrac{L_b - L_p}{L_r - L_p}\right)\right] \le M_p, & L_p < L_b \le L_r \\ F_{cr} S_x \le M_p, & L_b > L_r \end{cases} \tag{11}$$

Spec. Eq. F2-1
Spec. Eq. F2-2
Spec. Eq. F2-3

$$F_{cr} = \frac{C_b \pi^2 E}{\left(L_b/r_{ts}\right)^2}\sqrt{1 + 0.078\frac{Jc}{S_x h_0}\left(\frac{L_b}{r_{ts}}\right)^2} \tag{12}$$

Spec. Eq. F2-4

API RP-2A WSD (2014) Tubular Capacity Equations

In the second code check example, the 2D portal frame jacket, the tubular portal frame columns will be checked using the stability methods listed in Table 2, with the tubular capacity equations taken from API. The tubular beam-column interaction equations are given by API RP-2A WSD as:

$$\frac{f_a}{F_a} + \frac{C_m\sqrt{f_{bx}^2 + f_{by}^2}}{\left(1 - \dfrac{f_a}{F_e'}\right)F_b} \le 1.0 \tag{13}$$

6.20

$$\frac{f_a}{0.6F_y} + \frac{\sqrt{f_{bx}^2 + f_{by}^2}}{F_b} \le 1.0 \tag{14}$$

6.21

The axial allowable stress is identical to Equation 3. The tubular flexural allowable stress is as follows:

$$F_b, \text{ksi} = \begin{cases} 0.75F_y, & \dfrac{D}{t} \le \dfrac{1{,}500}{F_y} \\ \left(0.84 - 1.74\dfrac{F_y D}{Et}\right)F_y, & \dfrac{1{,}500}{F_y} < \dfrac{D}{t} \le \dfrac{3{,}000}{F_y} \\ \left(0.72 - 0.58\dfrac{F_y D}{Et}\right)F_y, & \dfrac{3{,}000}{F_y} < \dfrac{D}{t} \le 300 \end{cases} \tag{15}$$

6.6
6.7
6.8

where D is the outer diameter and t is the thickness of the tube. The similarities of beam-column interaction and axial allowable stress between the API RP-2A WSD and the 1989 AISC *Specification* indicate that the API equations and its frame stability method were formulated based on the 1989 *Specification* or prior.

DESIGN EXAMPLE 1

Given:

Perform the code checks for a cantilever W14×82 column 15 ft in length. Minor-axis column buckling is fully braced, with the code check performed in the major-axis direction. Use $K = 2.0$, $C_b = 1.67$, and $C_m = 0.85$. The loading is as follows:

$P = 300$ kips ($\beta = 2\%$)

$P = 210$ kips ($\beta = 5\%$)

Solution:

The geometric and material properties of the column are:

W14×82
$A_g = 24.0$ in.^{2}
$I_x = 881$ in.^{4}
$S_x = 123$ in.^{3}
$r_x = 6.06$ in.
$E = 29{,}000$ ksi

The cantilever is schematically shown in Figure 2. The first-order moment, the second-order P-Δ moment, and the second-order P-δ moment are illustrated in the same figure for the $H = 2\%P$ case. Note that the moments as shown have been magnified by the α factor. The purpose of this factor will be discussed in the following.

Load and Deflection Analyses

First-Order Load and Deflection

The first-order moment at the cantilever base is the top horizontal load multiplied by the height of the cantilever, $M_r = (\beta P)L$.

For the $H = 5\%P$ case,

$$\begin{aligned} M_r &= 5\%(210 \text{ kips})(15 \text{ ft}) \\ &= 158 \text{ kip-ft} \end{aligned}$$

For the $H = 2\%P$ case,

$$\begin{aligned} M_r &= 2\%(300 \text{ kips})(15 \text{ ft}) \\ &= 90 \text{ kip-ft} \end{aligned}$$

The selection of the axial loads, P, for these two cases is such that the unity checks result in approximately 0.90 for both cases.

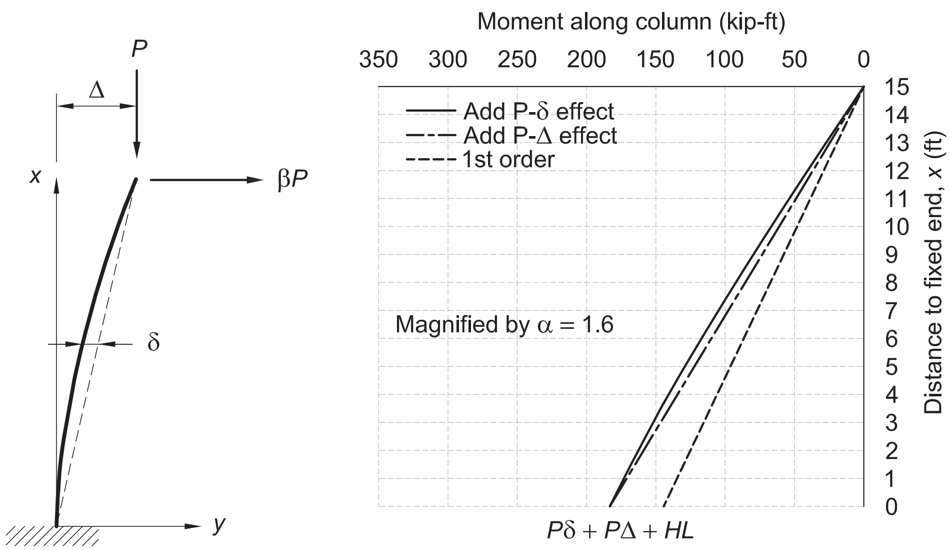

Fig. 2. Cantilever and moment distribution along member length.

The cantilever top deflection, for the case of $H = 2\%P$, can be calculated as:

$$\begin{aligned}\Delta_{1st} &= \frac{\alpha(\beta P)L^3}{3EI}\\ &= \frac{1.6(0.02)(300\text{ kips})(15\text{ ft})^3}{3(29{,}000\text{ ksi})(881\text{ in.}^4)}\\ &= 0.731\text{ in.}\end{aligned}$$

Note that an α factor of 1.6 was used in the deflection calculation. This is due to the requirement that the second-order effect needs to be assessed under the "factored" load. If LRFD is considered, $\alpha = 1.0$; $\alpha = 1.6$ for ASD or WSD. The deflection of 0.731 in., although a first-order value, will be used to assess the second-order effect.

Second-Order Load and Deflection

Geometric nonlinear beam-column analysis provides the second-order deflection along the cantilever height (see McGuire et. al., 2014):

$$y(x) = \frac{\beta}{\sqrt{\frac{\alpha P}{EI}}\cos\left(\sqrt{\frac{\alpha P}{EI}}L\right)}\sin\left(\sqrt{\frac{\alpha P}{EI}}x\right) - \beta x \tag{16}$$

The cantilever top deflection, for the case of $H = 2\%P$, is:

$$\begin{aligned}\sqrt{\frac{\alpha P}{EI}} &= \sqrt{\frac{1.6(300\text{ kips})}{(29{,}000\text{ ksi})(881\text{ in.}^4)}}\\ &= 4.33\times10^{-3}\text{ in.}^{-1}\end{aligned}$$

$$\begin{aligned}\Delta_{2nd} &= 2\%\frac{\sin\left[(4.33\times10^{-3}\text{ in.}^{-1})(15\text{ ft})\right]}{(4.33\times10^{-3}\text{ in.}^{-1})\cos\left[(4.33\times10^{-3}\text{ in.}^{-1})(15\text{ ft})\right]} - 2\%(15\text{ ft})\\ &= 0.967\text{ in.}\end{aligned}$$

Because the second-order base moment is the combination of $\beta(\alpha P)L + (\alpha P)\Delta_{2nd}$, this moment is calculated to be:

$$\begin{aligned}M_r &= \frac{(0.02)(1.6)(300\text{ kips})(15\text{ft}) + (1.6)(300\text{ kips})(0.967\text{ in.})}{1.6}\\ &= 114\text{ kip-ft}\end{aligned}$$

Note that the deflection and second-order effect are assessed at the αP level. The load and/or moment are first calculated under this factored condition, and then divided by α for code checks.

The parameter B_2 is an important indicator of the intensity of the second-order effect. This has been implied in Table 2, in which $B_2 = 1.5$ is used as a validity threshold on many of the frame stability calculation methods. B_2 is defined as the ratio between second- to first-order frame deflections. Hence, for the case of $H = 2\%P$, the B_2 factor is:

$$\begin{aligned}B_2 &= \frac{\Delta_{2nd}}{\Delta_{1st}}\\ &= \frac{0.967\text{ in.}}{0.731\text{ in.}}\\ &= 1.32\end{aligned}$$

In lieu of performing a second-order structural analysis, AISC provides an approximate estimate of B_2 that requires only a first-order structural analysis. This approximate formula is:

$$B_2 = \frac{1}{1 - \dfrac{\alpha P_{story}}{P_{e\,story}}} \tag{17}$$

where $P_{e\,story}$ is the estimate of story elastic critical buckling strength, expressed as:

$$\begin{aligned} P_{e\,story} &= R_m \frac{HL}{\Delta_{1st}} \\ &= 0.85\left[\frac{1.6(2\%)(300 \text{ kips})(15 \text{ ft})}{(0.731 \text{ in.})}\right] \\ &= 2{,}010 \text{ kips} \end{aligned}$$

This is compared to the classical Euler buckling load for the cantilever:

$$\begin{aligned} P_{cr} &= \frac{\pi^2 EI}{(KL)^2} \\ &= \frac{\pi^2(29{,}000 \text{ ksi})(881 \text{ in.}^4)}{\left[2.0(15 \text{ ft})\right]^2} \\ &= 1{,}950 \text{ kips} \end{aligned}$$

This indicates that $P_{e\,story}$ is a good approximation of P_{cr}. $P_{e\,story}$ applies to frames with more complex geometries other than cantilevers. It should be noted that $P_{e\,story}$ is a floor buckling concept—that is, when a floor with multiple columns reaches its buckling capacity. When assessing frame stability, $P_{e\,story}$ is more relevant as a capacity indicator than the individual column P_{cr}.

Substituting $P_{e\,story}$ into Equation 17,

$$\begin{aligned} B_2 &= \frac{1}{1 - \dfrac{1.6(300 \text{ kips})}{(2{,}010 \text{ kips})}} \\ &= 1.31 \end{aligned}$$

This is compared to the analytical B_2 of 1.32 calculated previously based on the deflection definition, and again this shows good agreement. AISC 360-16, Appendix 8, also provides an approximation to the second-order loads as follows:

$$\begin{aligned} P_r &= P_{nt} + B_2 P_{lt} \\ M_r &= B_1 M_{nt} + B_2 M_{lt} \end{aligned} \tag{18}$$

P_{nt} and M_{nt} are the member axial load and moment under only the vertical load, in which the subscript *nt* stands for "no-translation." P_{lt} and M_{lt} are the member axial load and moment under only the horizontal load, in which the subscript *lt* stands for "lateral-translation." P_{nt}, M_{nt}, P_{lt}, and M_{lt} are all obtained from the first-order analysis.

$$\begin{aligned} P_r &= P_{nt} + B_2 P_{lt} \\ &= (300 \text{ kips}) + 1.31(0 \text{ kips}) \\ &= 300 \text{ kips} \end{aligned}$$

$$\begin{aligned} M_r &= B_1 M_{nt} + B_2 M_{lt} \\ &= B_1(0 \text{ kip-ft}) + 1.31(0.02)(300 \text{ kips})(15 \text{ ft}) \\ &= 118 \text{ kip-ft} \end{aligned}$$

Table 4. First- and Second-Order Loads for the Cantilever Example			
	P_r (kips)	M_r (kips-ft)	B_2
H* = 5%*P			
First order	210	158	—
Second order	210	185	1.21
H* = 2%*P			
First order	300	90	—
Second order	300	114	1.32

These are compared to the second-order analytical results of $P_r = 300$ kips and $M_r = 114$ kip-ft from the previous calculations based on actual loads. This close agreement demonstrates the usefulness of the $B_1 - B_2$ method.

Designers have the choice of using structural software to automatically calculate the second-order responses. The designer can also opt for obtaining the first-order responses first and then applying the $B_1 - B_2$ method. This $B_1 - B_2$ method is quite versatile and applies to structures with more complex geometries than a simple cantilever. However, for offshore structures with several open frames (e.g., portal frame plus several unbraced topsides module-support structures), it may be difficult to efficiently perform the $B_1 - B_2$ analysis method.

Even if the designers choose to perform a full second-order computer analysis, it is important for them to be aware of this simplified $B_1 - B_2$ method in order to check their computer results. The first- and second-order loads required for further cantilever code checks are summarized in Table 4.

Case of $H = 5\%P$

Code Check Using the 1989 AISC Specification

The following load demands at the cantilever base are taken from Table 4. Referring to Table 1, it is noted that the first-order loads need to be used with the 1989 *Specification* check.

$$P_r = 210 \text{ kips}$$
$$M_r = 158 \text{ kip-ft}$$

The applied axial and bending stresses are then as follows:

$$\begin{aligned} f_a &= \frac{P_r}{A_g} \\ &= \frac{210 \text{ kips}}{24 \text{ in.}^2} \\ &= 8.75 \text{ ksi} \end{aligned}$$

$$\begin{aligned} f_b &= \frac{M_r}{S_x} \\ &= \frac{158 \text{ kip-ft}}{123 \text{ in.}^2} \\ &= 15.3 \text{ ksi} \end{aligned}$$

The allowable axial and bending stresses are calculated using Equations 3, 4, and 6. The AISC *Steel Construction Manual* (2017) provides many convenient charts and tables where these capacities can be efficiently evaluated. Hence, we will not provide the calculation details. The capacity values are directly provided here:

$$F_a = 22.8 \text{ ksi}$$
$$F_b = 30 \text{ ksi}$$

The following factored Euler buckling stress is also required for code checks:

$$
\begin{aligned}
F_e' &= \frac{12\pi^2 E}{23(KL/r)^2} \\
&= \frac{12\pi^2(29{,}000\text{ ksi})}{23\left[(2.0)(15\text{ ft})/(6.06\text{ in.})\right]^2} \\
&= 42.3\text{ ksi}
\end{aligned}
$$

The 1989 *Specification* unity check value is thus calculated as:

$$
\begin{aligned}
\frac{f_a}{F_a} + \frac{C_m f_b}{\left(1-\dfrac{f_a}{F_e'}\right)F_b} &= \frac{8.75\text{ ksi}}{22.8\text{ ksi}} + \frac{0.85(15.4\text{ ksi})}{\left(1-\dfrac{8.75\text{ ksi}}{42.3\text{ ksi}}\right)(30\text{ ksi})} \\
&= 0.932
\end{aligned}
$$

Code Check Using the AISC 360-16 ELM

The load demands at the base of the cantilever are taken from Table 4. Note that the second-order loads need to be used with AISC 360-16.

$$
\begin{aligned}
P_r &= 210\text{ kips} \\
M_r &= 185\text{ kip-ft}
\end{aligned}
$$

The nominal axial and flexural strengths are calculated, based on Equations 9 and 11, to be $P_n = 927$ kips and $M_n = 579$ kip-ft. As mentioned earlier, standard charts and tables exist for fast capacity calculations; thus their details are not provided here. To be used for ASD, these nominal strengths are reduced by the ASD safety factor, Ω_c:

$$
\begin{aligned}
P_c &= \frac{P_n}{\Omega_c} \\
&= \frac{927\text{ kips}}{1.67} \\
&= 555\text{ kips}
\end{aligned}
$$

$$
\begin{aligned}
M_c &= \frac{M_n}{\Omega_c} \\
&= \frac{579\text{ kip-ft}}{1.67} \\
&= 347\text{ kip-ft}
\end{aligned}
$$

Because $P_r/P_c > 0.2$, the AISC 360-16 unity check value is:

$$
\begin{aligned}
\frac{P_r}{P_c} + \frac{8}{9}\left(\frac{M_r}{M_c}\right) &= \frac{210\text{ kips}}{555\text{ kips}} + \frac{8}{9}\frac{(185\text{ kip-ft})}{(347\text{ kip-ft})} \\
&= 0.852
\end{aligned}
$$

Case of $H = 2\%P$

***Code Check Using the 1989 AISC* Specification**

The load demands at the base of the cantilever are taken from Table 4:

$$
\begin{aligned}
P_r &= 300\text{ kips} \\
M_r &= 90\text{ kip-ft}
\end{aligned}
$$

The applied axial and bending stresses are then calculated as follows:

$$
\begin{aligned}
f_a &= \frac{P_r}{A_g} \\
&= \frac{300 \text{ kips}}{24 \text{ in.}^2} \\
&= 12.5 \text{ ksi}
\end{aligned}
$$

$$
\begin{aligned}
f_b &= \frac{M_r}{S_x} \\
&= \frac{90 \text{ kip-ft}}{123 \text{ in.}^2} \\
&= 8.78 \text{ ksi}
\end{aligned}
$$

The allowable axial and bending stresses, as well as the factored Euler stress, are identical to the $H = 5\%P$ case—that is:

$$
\begin{aligned}
F_a &= 22.8 \text{ ksi} \\
F_b &= 30 \text{ ksi} \\
F'_e &= 42.3 \text{ ksi}
\end{aligned}
$$

The 1989 *Specification* code unity check value is thus calculated as:

$$
\begin{aligned}
\frac{f_a}{F_a} + \frac{C_m f_b}{\left(1 - \frac{f_a}{F'_e}\right) F_b} &= \frac{12.5 \text{ ksi}}{22.8 \text{ ksi}} + \frac{0.85(8.78 \text{ ksi})}{\left(1 - \frac{8.75 \text{ ksi}}{42.3 \text{ ksi}}\right)(30 \text{ ksi})} \\
&= 0.901
\end{aligned}
$$

Code Check Using the AISC 360-16 ELM

The load demands at the base of the cantilever are taken from Table 4:

$$
\begin{aligned}
P_r &= 300 \text{ kips} \\
M_r &= 114 \text{ kip-ft}
\end{aligned}
$$

As with the $H = 5\%P$ case, the nominal axial and flexural strengths are calculated, based on Equations 9 and 11, to be $P_n =$ 927 kips and $M_n = 579$ kip-ft. To be used for ASD, these nominal strengths are reduced by the ASD safety factor Ω_c:

$$
\begin{aligned}
P_c &= \frac{P_n}{\Omega_c} \\
&= \frac{927 \text{ kips}}{1.67} \\
&= 555 \text{ kips}
\end{aligned}
$$

$$
\begin{aligned}
M_c &= \frac{M_n}{\Omega_c} \\
&= \frac{579 \text{ kip-ft}}{1.67} \\
&= 347 \text{ kip-ft}
\end{aligned}
$$

Table 5. Unity Check Ratios for the Cantilever Example		
	1989 *Specification*	AISC 360-16
$H = 5\%P$	0.932	0.852 (–8.6%)
$H = 2\%P$	0.901	0.832 (–7.7%)
Note: % change is measured against the 1989 *Specification* UC value.		

Because $P_r/P_c > 0.2$, the AISC 360-16 code check value is:

$$\frac{P_r}{P_c}+\frac{8}{9}\left(\frac{M_r}{M_c}\right)=\frac{300\text{ kips}}{555\text{ kips}}+\frac{8}{9}\frac{(114\text{ kip-ft})}{(347\text{ kip-ft})}$$
$$=0.832$$

Unity Check Summary for the Cantilever Example

The code unity check (UC) values for the cantilever example are summarized in Table 5. For the $H = 5\%P$ case, bending has a larger UC component than axial force. For the $H = 2\%P$ case, the situation is reversed with the axial force having a larger UC component than bending. However, this has only a minor effect on the relative UC between the 1989 AISC *Specification* and AISC 360-16, as shown in Table 5. The AISC 360-16 UC values are lower than the 1989 *Specification* values by approximately 8%. This is first because the 1989 *Specification* flexural capacity is typically lower than AISC 360-16. The 360-16 flexure strength considers the combination of torsional and warping rigidities, while the 1989 *Specification* only considers the larger of the two. The second reason that 360-16 tends to be lower is due to the 8/9 factor in Equation 7. In the 1989 *Specification* beam-column buckling equation, Equation 1, this factor does not exist.

DESIGN EXAMPLE 2

Given:

Perform code checks for the 2D jacket structure, as shown in Figure 3, at the top of a portal tubular column where the highest bending moment occurs. The tubular column has the following geometric and material properties:

36 in. × 1 in.
A_g = 110 in.^{2}
I = 16,851 in.^{4}
S = 936 in.^{3}
r = 12.3 in.
E = 29,000 ksi
F_y = 50 ksi
L = 33 ft

The following parameters also apply to the column:

K = 1.8 (AISC *Manual*, 9th Ed, ELM)
K = 1.0 (DM, FOM)
C_m = 0.85

The column loading is as follows:

P = 2,600 kips
q = 4 kips/ft
Total vertical load $V = P + 2q$ (74.7 ft)
Total horizontal load $H = 2\%V$

The portal frame columns are tubular members; hence, API RP-2A provisions will be used in their design. The code checks to be performed are thus not truly AISC *Specification* checks but are similar. In API RP-2A, the analysis approach and beam-column resemble the AISC *Specification* equations, but the tubular allowable stresses are taken from the API RP-2A WSD provisions.

A Note on the *K*-Factor

A recently published paper by Ku et. al. (2020) discussed the various *K*-factor calculation procedures for portal frame columns. For the 2D structure considered in this example, the portal column *K*-factor has the following values from different analysis methods:

AISC *Specification* unbraced alignment chart:	$K = 2.45$
Ku et. al. (2020):	$K = 1.69$
ABAQUS FEM Solution:	$K = 1.78$

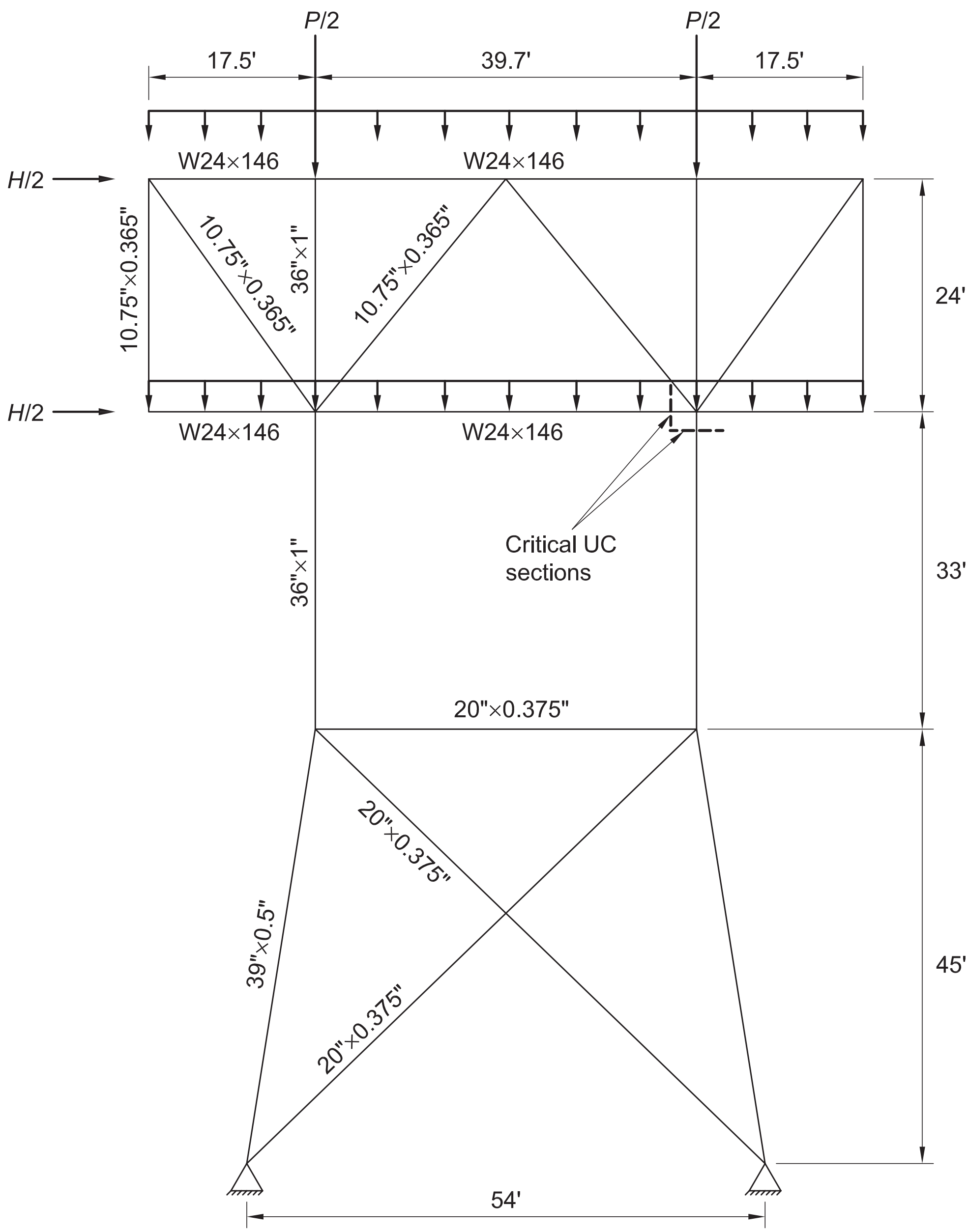

Fig. 3. Two-dimensional offshore jacket.

Table 6. First- and Second-Order Loads for the 2D Jacket Example ($H = 2\%V$)			
	P_r (kips)	M_r (kip-ft)	B_2
First order	1,650	642	—
Second order (ELM)	1,660	808	1.35
Second order (DM)	1,660	869	1.41
First order (FOM)	1,660	897	—

The AISC *Specification* unbraced alignment chart applies to a moment frame, which is completely unbraced throughout the height of structure. For a jacket portal frame, it is combined with a braced topside from above and a braced jacket from below. Thus, the assumption of a complete moment frame results in a K-factor that is too conservative. Ku et. al (2020) provides a new analytical K-factor solution based on the braced-unbraced-braced configuration. This analytical solution was derived by using slope-deflection equations coupled with stability functions that results in an improved K-factor estimate for portal columns. In the following, $K = 1.8$ will be used in all code checks that require a K-factor (i.e., $K \neq 1$).

Load Analysis

The general-purpose finite element analysis software ABAQUS (2018) was used to determine the first- and second-order member loads and joint deflections. Each of the portal frame columns is discretized into eight 2-node beam-column elements. Other structural components of the 2D topsides and jackets are discretized with meshes of similar size.

The portal column loads from the ABAQUS analyses are shown in Table 6. For the second-order analysis, the external loads need to be magnified by the $\alpha = 1.6$ factor for response calculations. The member loads thus obtained are then divided by the α factor for member code checks. In lieu of second-order analysis, the $B_1 - B_2$ method coupled with first-order structural analysis can also be used to obtain the second-order loads. Accurate second-order loads similar to the Table 6 numbers can be obtained from the $B_1 - B_2$ method; see IntelliSIMS (2019a, b).

First-Order Load

The first-order column loads are obtained from the first-order structural analysis using nominal EA and EI, with the external loads given in Figure 3.

Second-Order (ELM) Load

The second-order ELM column loads are obtained from the second-order structural analysis using nominal EA and EI, with the external loads given in Figure 3 multiplied by $\alpha = 1.6$. After the second-order structural analysis, the resulting member loads are divided by $\alpha = 1.6$ and used for design. With reference to Table 2, the ELM method can only be used when $B_2 \leq 1.5$. This is confirmed by Table 6 in which the B_2 factor is calculated as 1.35. Also, from Table 2, a minimum notional load of $0.2\%V$ needs to be considered. Because the actual lateral load applied is $2\%V$, this minimum notional lateral load does not apply.

Second-Order (DM) Load

The second-order DM column loads are obtained from the second-order structural analysis using $0.8EA$ and $0.8EI$, with the external loads given in Figure 3 multiplied by $\alpha = 1.6$. After the second-order structural analysis, the resulting member loads are divided by $\alpha = 1.6$ and used for design. The following portal column axial load ratio is checked:

$$\frac{\alpha P_r}{P_y} = \frac{1.6(1{,}660 \text{ kips})}{(50 \text{ ksi})(110 \text{ in.}^2)}$$
$$= 0.48 \leq 0.50$$

Hence, no further stiffness reduction of the portal columns is required; see Table 2. The minimum notional load of $0.2\%V$ does not apply since the actual lateral load is $2\%V$, for the case of $B_2 \leq 1.5$.

First-Order FOM Load

The first-order FOM column loads are obtained from the first-order structural analysis using nominal *EA* and *EI*, with the external loads given in Figure 3. An additional lateral load, N_i, must be applied at the top of the portal bay. N_i is calculated as:

$$
\begin{aligned}
N_i &= 2.1\left(\frac{\Delta}{L}\right)Y_i \\
&= 2.1\left(\frac{1.1\text{ in.}}{33\text{ ft}}\right)(3{,}200\text{ kips}) \\
&= 29.8\text{ kips}
\end{aligned}
$$

where Δ is the first-order portal frame interstory drift under the external load in Figure 3, $L = 33$ ft is the portal column length, and Y_i is the total vertical load applied at the portal column bay. $Y_i = V$ in this example. This lateral load, N_i, is "additive"; that is, it needs to apply regardless of the magnitude of actual lateral load. From Table 2, N_i also needs to be checked for:

$$N_i \geq 0.0042\frac{Y_i}{\alpha}$$

$$N_i = 29.8\text{ kips}$$

$$
\begin{aligned}
0.0042\frac{Y_i}{\alpha} &= 0.0042\frac{(3{,}200\text{ kips})}{1.6} \\
&= 8.39\text{ kips}
\end{aligned}
$$

which is satisfied.

Validity of the FOM method is limited to cases with member axial load $\alpha P_r/P_y \leq 0.50$. This value was calculated earlier as 0.48; thus, the FOM method can be used. It has been mentioned earlier in this paper that the $H = 5\%V$ case is more likely to be the norm for offshore structures, in which the axial load demand is less than the $H = 2\%V$ case. Because the $H = 2\%V$ case just barely passed the FOM applicability threshold, it can be reasonably expected that the FOM method may be applicable to most offshore structures. The offshore structural designers need to fully understand the various applicability conditions before applying the different stability methods listed in Table 2.

Case of $H = 2\%V$

Code Check Based on the 1989 Specification

The load demands at the top of the portal column are taken from Table 6. Note that the first-order loads need to be used with the 1989 *Specification* check.

$$P_r = 1{,}650\text{ kips};\ M_r = 642\text{ kip-ft}$$

The applied axial and bending stresses are then as follows:

$$
\begin{aligned}
f_a &= \frac{P_r}{A_g} \\
&= \frac{1{,}650\text{ kips}}{110\text{ in.}^2} \\
&= 15.0\text{ ksi}
\end{aligned}
$$

$$
\begin{aligned}
f_b &= \frac{M_r}{S} \\
&= \frac{642\text{ kip-ft}}{936\text{ in.}^2} \\
&= 8.23\text{ ksi}
\end{aligned}
$$

The allowable axial and bending stresses were calculated using Equations 3 and 15:

$$F_a = 23.1 \text{ ksi}$$
$$F_b = 36.6 \text{ ksi}$$

The following factored Euler buckling stress is required for code checks:

$$\begin{aligned} F'_e &= \frac{12\pi^2 E}{23(KL/r)^2} \\ &= \frac{12\pi^2 (29{,}000 \text{ ksi})}{23\left[1.8(33 \text{ ft})/(12.3 \text{ in.})\right]^2} \\ &= 45.0 \text{ ksi} \end{aligned}$$

The 1989 *Specification* unity check value is thus calculated as follows:

$$\begin{aligned} \frac{f_a}{F_a} + \frac{C_m f_b}{\left(1 - \dfrac{f_a}{F'_e}\right) F_b} &= \frac{15.0 \text{ ksi}}{23.1 \text{ ksi}} + \frac{0.85(8.23 \text{ ksi})}{\left(1 - \dfrac{15 \text{ ksi}}{45.0 \text{ ksi}}\right)(36.6 \text{ ksi})} \\ &= 0.935 \end{aligned}$$

Code Check Using the AISC 360-16 ELM

The load demands at the top of the portal column are taken from Table 6. Note that the second order (ELM) loads are used.

$$P_r = 1{,}660 \text{ kips}$$
$$M_r = 808 \text{ kip-ft}$$

The allowable axial and bending stresses are identical to the 1989 *Specification* procedure, with the cross-sectional allowable strengths as:

$$F_a = 23.1 \text{ ksi}$$
$$F_b = 36.6 \text{ ksi}$$

$$\begin{aligned} P_c &= F_a A_g \\ &= (23.1 \text{ ksi})(110 \text{ in.}^2) \\ &= 2{,}540 \text{ kips} \end{aligned}$$

$$\begin{aligned} M_c &= F_b S \\ &= (36.6 \text{ ksi})(936 \text{ in.}^2) \\ &= 2{,}860 \text{ kip-ft} \end{aligned}$$

Because P_r/P_c = (1,660 kips)/(2,540 kips) = 0.653 > 0.2, the 360-16 *Specification* code check value is:

$$\begin{aligned} \frac{P_r}{P_c} + \frac{8}{9}\left(\frac{M_r}{M_c}\right) &= \frac{1{,}660 \text{ kips}}{2{,}540 \text{ kips}} + \frac{8}{9}\frac{(808 \text{ kip-ft})}{(2{,}860 \text{ kip-ft})} \\ &= 0.904 \end{aligned}$$

Code Check Using the AISC 360-16 DM

The load demands for the portal column are taken from Table 6. Note that the second order (DM) loads are used:

$P_r \;= 1{,}660$ kips

$M_r = 869$ kip-ft

The allowable axial and bending stresses for the DM method are as follows:

$F_a = 26.9$ ksi

$F_b = 36.6$ ksi

An important advantage of the DM method is that the K-factor can be taken as 1.0; see Table 2. This results in the axial allowable stress increase from 23.1 ksi to 26.9 ksi, illustrated in Figure 4.

Although the K-factor is reduced from 1.8 to 1.0, the increase in allowable stress is less dramatic. This is because for not-too-slender members, the axial capacity is controlled by plastic buckling—that is, a transition region from elastic buckling to full yield. In this region, the member capacity is less sensitive to the change of K-factors when compared to the elastic buckling region.

The allowable cross-sectional strengths are calculated as follows:

$$\begin{aligned} P_c &= F_a A_g \\ &= (26.9 \text{ ksi})(110 \text{ in.}^2) \\ &= 2{,}960 \text{ kips} \end{aligned}$$

$$\begin{aligned} M_c &= F_b S \\ &= (36.6 \text{ ksi})(936 \text{ in.}^3) \\ &= 2{,}860 \text{ kip-ft} \end{aligned}$$

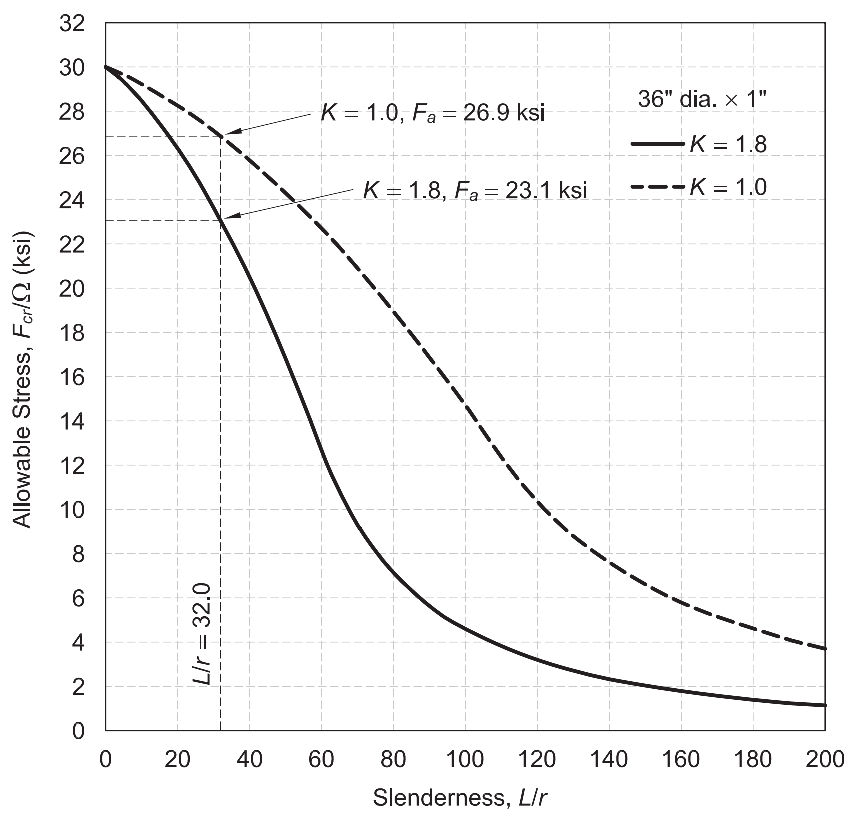

Fig. 4. Axial allowable stress comparison between ELM and DM.

Table 7. Code Unity Check Ratios for the 2-D Jacket Example (*H* = 2%*V*)	
	UC Values
1989 AISC *Specification* procedure	0.935
AISC 360-16 ELM procedure	0.904 (–3.3%)
AISC 360-16 DM procedure	0.833 (–10.9%)
AISC 360-16 FOM procedure	0.842 (–9.9%)
Note: % change measured against 1989 AISC *Specification* UC.	

Because P_r/P_c = (1,660 kips)/(2,960 kips) = 0.563 > 0.2, the AISC 360 DM code check value is:

$$\frac{P_r}{P_c}+\frac{8}{9}\left(\frac{M_r}{M_c}\right)=\frac{1{,}660\text{ kips}}{2{,}960\text{ kips}}+\frac{8}{9}\frac{(869\text{ kip-ft})}{(2{,}860\text{ kip-ft})}$$
$$=0.833$$

Code Check Using the AISC 360-16 FOM

The load demands at the top of the portal column are taken from Table 6. Note that the first-order (FOM) loads are used.

$$P_r = 1{,}660\text{ kips}$$
$$M_r = 897\text{ kip-ft}$$

The allowable stress and the allowable cross-sectional strengths are identical to the DM case (note that K = 1):

$$P_c = 2{,}960\text{ kips}$$
$$M_c = 2{,}860\text{ kip-ft}$$

Because P_r/P_c = (1,660 kips)/(2,960 kips) = 0.563 > 0.2, the 360-16 FOM code check value is:

$$\frac{P_r}{P_c}+\frac{8}{9}\left(\frac{M_r}{M_c}\right)=\frac{1{,}660\text{ kips}}{2{,}960\text{ kips}}+\frac{8}{9}\frac{(897\text{ kip-ft})}{(2{,}860\text{ kip-ft})}$$
$$=0.842$$

UC Summary for the 2D Jacket Example

Code unity check values are summarized in Table 7. The comparisons are consistent with the cantilever example of Table 5, with the AISC 360-16 ELM UC value slightly lower than the 1989 *Specification* value. The decrease in UC is slightly less when compared to the cantilever example (–3.3% vs. –7.7%). This can be attributed to the fact that for wide-flange members, the lateral-torsional buckling strength is almost always higher in AISC 360-16 than in the 1989 AISC *Specification*. For tubular members, this difference does not exist.

Further UC reduction from ELM to DM/FOM is also observed in Table 7. Other examples studied in IntelliSIMS (2019a, b) show similar trends. This can be attributed to the fact that the axial allowable stresses are higher in DM/FOM due to K = 1, while the bending moment increase (from reduced *EA* and *EI*) is relatively low and not enough to offset the axial allowable stress increase. The preceding observations apply to the relatively low B_2 range encountered for typical offshore structures. DM and FOM results are similar, which can be anticipated because FOM is, in fact, a calibrated simplified method from DM. Detailed explanations of this calibration can be seen, for example, in AISC Design Guide 28 (Griffis and White, 2013).

PLANNED AISC-360 ADOPTION PATH

The API AISC-360 Adoption Task Group has generated two technical reports (IntelliSIMS, 2019a, b) as well as training material. Both the technical reports and the training material were designed to raise the offshore industry's awareness on frame stability procedures between the 1989 and 2016 AISC *Specifications*. As discussed in the Introduction, although the API RP-2TOP has adopted AISC 360-10, the relationship between the first- and second-order structural analyses and their distinctly matched beam-column equations have not been fully explained in API RP-2TOP.

The tubular member design equations as contained in API RP-2A WSD and API RP-2A LRFD are based on methodologies consistent with the 1989 AISC *Specification*. The structural analysis is based on the first-order analysis, and the beam-column equation uses a magnification factor for the second-order effect. This governing practice for offshore structures is thus not compatible with AISC 360-16. Therefore, although API RP-2TOP adopts AISC 360, the offshore designers who wish to use RP-2TOP will need to perform both the first- and second-order analyses and then perform member checks in two separate groups (one group for tubular members, and the other for wide-flange and other nontubular members).

The path forward for the offshore structural industry is to continue raising the awareness of the compatibility issue of technical principles. In parallel, addendums and new revisions for API RP-2A and RP-2TOP should be planned to clarify the code check processes. It is envisioned that the frame stability process for the API RP-2A standards will be updated in the next revision for full compatibility with AISC 360.

CONCLUSION

API has discouraged the use of AISC *Specifications* in the past, and only recently (in 2019) partially adopted AISC 360-10 via the publication of API RP-2TOP for the topsides (i.e., deck) designs. The adoption is partial, as RP-2TOP is load and resistance factor design (LRFD) based and is tied to the simultaneously published API RP-2A LRFD 2nd Edition. The traditional method of offshore structural design for U.S. practices has been working stress design, and it will continue to dominate in the foreseeable future. The latest API RP-2A WSD has yet to adopt any AISC *Specification* later than 1989.

In this paper, two examples were discussed in detail regarding their load calculations and code check processes. This paper should be helpful to offshore structural engineers who wish to understand the AISC 360 frame stability procedure. In general, the AISC 360 stability procedure is easy to understand, and its three associated methods (the ELM, DM, and FOM) are straightforward to apply in practice. Structural code checks using the 1989 and 2016 AISC *Specifications* result in similar values, with the 1989 *Specification* slightly on the conservative side. This slight advantage on economy, when switching to the AISC 2016 *Specification*, in terms of weight savings perhaps will be a welcome news to a cost-conscious industry.

API formed a Task Group in 2019 assigned to study the issues associated with AISC 360 adoption. In the immediate future, this Task Group will likely be preparing addendums and/or revisions to existing standards, with the objective of eventual full compatibility with AISC 360.

ACKNOWLEDGMENTS

The authors would like to thank the remaining members of the API AISC-360 Adoption Task Group for their dedication: Boon Sze Tan, Ralph Shaw, Fu Wu, Ben Bialas, Geoff McDonald, Bernard Cyprian, Jay Hooper, Andrea Mangiavacchi, Ian Chu, and Zhaoji Wang. The authors would also like to thank API for the funding it provided to support this study. The opinions expressed in this paper are those of the authors and do not necessarily reflect API's official position.

REFERENCES

ABAQUS/CAE (2018), Dassault Systems Simulia Corp., Johnston, R.I.

AISC (1986), *Load and Resistance Factor Design Specification for Structural Steel Buildings*, American Institute of Steel Construction, Chicago, Ill.

AISC (1989a), *Specification for Structural Steel Buildings, Allowable Stress Design and Plastic Design*, American Institute of Steel Construction, Chicago, Ill.

AISC (1989b), *Steel Construction Manual*, 9th Ed., American Institute of Steel Construction, Chicago, Ill.

AISC (2010), *Specification for Structural Steel Buildings*, ANSI/AISC 360-10, American Institute of Steel Construction, Chicago, Ill.

AISC (2011), *Steel Construction Manual*, 14th Ed., American Institute of Steel Construction, Chicago, Ill.

AISC (2016), *Specification for Structural Steel Buildings*, ANSI/AISC 360-16, American Institute of Steel Construction, Chicago, Ill.

AISC (2017), *Steel Construction Manual*, 15th Ed., American Institute of Steel Construction, Chicago, Ill.

API (1969), *Recommended Practice for Planning, Designing, and Constructing Fixed Offshore Platforms*, 1st Ed., American Petroleum Institute, Washington, D.C.

API (1993), *Recommended Practice 2A-LRFD, Planning, Designing, and Constructing Fixed Offshore Platforms—Load and Resistance Factor Design*, 1st Ed., American Petroleum Institute, Washington, D.C.

API (2014), *Recommended Practice 2A-WSD, Planning, Designing, and Constructing Fixed Offshore Platforms—Working Stress Design*, 22nd Ed., American Petroleum Institute, Washington, D.C.

API (2019), *Recommended Practice 2A-LRFD, Planning, Designing, and Constructing Fixed Offshore Platforms—Load and Resistance Factor Design*, 2nd Ed., American Petroleum Institute, Washington, D.C.

ANSI/API (2019), *Recommended Practice 2TOP*, 1st Ed., ISO 19901-3:2010 (Modified), Petroleum and Natural Gas Industries—Specific Requirements for Offshore Structures—Part 3: Topsides Structure, American Petroleum Institute, Washington, D.C.

Bernuzzi, C., Cordova, B., and Simoncelli, M. (2015), "Unbraced Steel Frame Design According to EC3 and AISC Provisions," *Journal of Constructional Steel Research*, Vol. 114, pp. 157–177.

Carter, C. (2013), *The Evolution of Stability Provisions in the AISC Specification*, SteelDay Eve Presentation, AISC Education Archives, www.aisc.org.

Carter, C. and Geschwindner, L. (2008), "A Comparison of Frame Stability Analysis Methods in ANSI/AISC 360-05," *Engineering Journal*, AISC, Vol. 45, No. 3, pp. 159–170.

Griffis, L.G. and White, D.W. (2013), *Stability Design of Steel Buildings*, Design Guide 28, AISC, Chicago, Ill.

IntelliSIMS (2019a), *AISC-360 Adoption Phase 1 Report*, A Report for API, Revision B.

IntelliSIMS (2019b), *AISC-360 Adoption Phase 2 Report*, A Report for API, Revision A.

Ku, A., Chen, J., and Gunzelman S. (2020), "K-Factor Solution for Combined Braced-Unbraced Offshore Jacket Frames," *Journal of Offshore Mechanics and Arctic Engineering*, Vol. 142, pp. 021703-1-6.

McGuire, W., Gallagher, R.H., and Ziemian, R.D. (2014), *Matrix Structural Analysis*, 2nd Ed., John Wiley & Sons, Inc., New York, N.Y.

Ziemian, R.D. (ed.) (2010), *Guide to Stability Design Criteria for Metal Structures*, 6th Ed., John Wiley & Sons, Inc., Hoboken, N.J.